

X-ray reflection in a sample of X-ray bright Ultraluminous X-ray sources

M. D. Caballero-García^{1*} and A. C. Fabian¹

¹*Institute of Astronomy, Madingley Road, Cambridge, CB3 0HA*

ABSTRACT

We apply a reflection-based model to the best available *XMM-Newton* spectra of X-ray bright UltraLuminous X-ray (ULX) sources (NGC 1313 X–1, NGC 1313 X–2, M 81 X–6, Holmberg IX X–1, NGC 5408 X–1 and Holmberg II X–1). A spectral drop is apparent in the data of all the sources at energies 6–7 keV. The drop is interpreted here in terms of relativistically-blurred ionized reflection from the accretion disk. A soft-excess is also detected from these sources (as usually found in the spectra of AGN), with emission from O K and Fe L, in the case of NGC 5408 X–1 and Holmberg II X–1, which can be understood as features arising from reflection of the disk. Remarkably, ionized disk reflection and the associated powerlaw continuum provide a good description of the broad-band spectrum, including the soft-excess. There is no requirement for thermal emission from the inner disk in the description of the spectra. The black holes of these systems must then be highly spinning, with a spin close to the maximum rate of a maximal spinning black hole. The results require the action of strong light bending in these sources. We suggest that they could be strongly accreting black holes in which most of the energy is extracted from the flow magnetically and released above the disc thereby avoiding the conventional Eddington limit.

Key words: line: formation – black hole physics – X-rays: galaxies – X-rays: general

1 INTRODUCTION

Ultra-luminous X-ray (ULX) sources are point like, nonnuclear sources observed at other galaxies, with observed luminosities greater than the Eddington luminosity for a $10 M_{\odot}$ stellar mass black hole (BH), with $L_X \geq 10^{39} \text{ erg s}^{-1}$ (Fabbiano 1989). The true nature of these objects is still open to debate (Miller & Colbert 2004). One fundamental issue is whether the emission is isotropic or beamed along our line-of-sight. A possible scenario for geometrical beaming involves super-Eddington accretion during phases of thermal-timescale mass transfer (King 2002). Alternatively, if the emission is isotropic and the Eddington limit is not violated, ULX must be fuelled by accretion onto Intermediate-Mass BH (IMBH), with masses in the range $100\text{--}10\,000 M_{\odot}$ (Colbert & Mushotzky 1999). Currently, there is no agreement regarding the nature of these sources. It is possible that some ULX appear very luminous because of a combination of moderately high mass, mild beaming and mild super-Eddington emission. It is also possible that ULX are an inhomogeneous population, comprised of both a subsample of IMBH and moderately beamed stellar mass black holes (Fabbiano & White 2006; Miller & Colbert 2004).

NGC 5408 X–1, HOLM II X–1, M 81 X–9 (which is in the companion-dwarf galaxy Holmberg IX, hereafter called HOLM IX X–1), the ULX in NGC 1313 and M 81 X–6 are ULX located

in dwarf (NGC 5408 X–1, HOLM II X–1 and HOLM IX X–1) and spiral (NGC 1313 X–1, NGC 1313 X–2 and M 81 X–6) galaxies, respectively. All these ULX peak in X-ray luminosity above $L_X = 1 \times 10^{40} \text{ erg s}^{-1}$, thus being excellent targets for testing spectral models to the data. They are nearby and located at distances of $D = 4.8, 3.5, 3.7, 3.63, 4.50 \text{ Mpc}$ (Karachentsev 2002; Stobbart et al. 2006; Liu & Di Stefano 2008), for NGC 5408 X–1, HOLM IX X–1, NGC 1313 X–1, M 81 X–6 and HOLM II X–1 respectively. NGC 5408 X–1 is among the few ULX for which (10–200 mHz) Quasi-Periodic Oscillations (QPO) have been found (Strohmayer et al. 2007; Dewangan et al. 2006). NGC 5408 X–1 exhibits X-ray timing and spectral properties analogous to those exhibited by Galactic stellar-mass black hole in the *very high or steep power-law* state (Remillard & McClintock 2006), but with the characteristic variability timescales (QPO and break frequencies) consistently scaled down (Strohmayer et al. 2007). For NGC 5408 X–1 the inferred characteristic size for the X-ray emitting region is ≈ 100 times larger than the typical inner disk radii of Galactic black holes. The highest signal-to-noise spectra of ULX can often be fitted by composite models of a thermal disk together with a hard-powerlaw tail, with a low measured disk temperature of $\approx 0.2 \text{ keV}$ (Miller et al. 2003, 2004). If such factors are entirely due to a higher black hole mass, they imply an IMBH with $M \approx 100\text{--}10\,000 M_{\odot}$. Both the morphology and flux of the optical high-excitation nebulae detected around some ULX probably rule out strong beaming as the origin of the X-ray emission (Pakull & Mirioni 2003; Kaaret et al. 2004; Soria et al. 2006; Abolmasov et al. 2007).

* E-mail: mcaballe@ast.cam.ac.uk

The detection for most ULX of spectral curvature, in the form of a deficit of photons at energies $E \geq 2$ keV (Roberts et al. 2005; Stobbart et al. 2006; Miyawaki et al. 2009) has led to the suggestion that most ULX have spectral properties that do not correspond to any of the accretion states known in Black Hole Binaries (BHB), making it unlikely that ULX are powered by sub-Eddington flows onto an IMBH (Roberts et al. 2007). The application of Comptonization models to the data (Stobbart et al. 2006; Gladstone et al. 2009 and references therein) results in strikingly high and low values for the coronal opacity ($\tau \geq 5$) and the electron temperature ($kT_e = 1 - 3$ keV), difficult to explain for the expected physical conditions in a corona surrounding the black hole. This is very different to the typical values found for BHB during the *low/hard* state, with spectra dominated by Comptonization¹, and appears irreconcilable with the IMBH model, which assumes that they operate as simple scaled-up BHB.

Here, we present an alternative interpretation of the spectral shape, based on a physically-justified model commonly used on other accreting black holes. The soft part of the spectrum ($E \leq 1$ keV) – the soft X-ray excess – and the high-energy curvature are just aspects of a reflection spectrum expected from accretion (Guilbert & Rees 1988; George & Fabian 1991). A major component of reflection, the broad iron K line, has been found in many Seyfert galaxies (Tanaka et al. 1995; Nandra et al. 2008), accreting stellar-mass black holes (Miller et al. 2007; Reis et al. 2009a) and even accreting neutron stars (Cackett et al. 2008; Reis et al. 2009b). Both the soft excess and the relativistic broad iron K line have recently been demonstrated to be part of the same physical process, i.e., the reaction of the disk to irradiation from a high-energy source, in the Seyfert-1 galaxy 1H 0707-495 (Fabian et al. 2009). In this paper we investigate whether reflection models can account for the spectra of these ULX and, if so, we put them in the context of the accreting black holes known so far.

For this study, we choose the ULX with the best available data and with the longest exposure time observations (≈ 100 ks of exposure time) of the *XMM-Newton* satellite. By using only the highest quality data from the widest band pass, highest sensitivity instruments available we expect to make good statements on the accretion processes in these ULX. In Section 2 we describe the observations and data used, in Section 3 we report on the results of the application of fits with the reflection model to the spectra and in Section 4 discuss the results obtained.

2 OBSERVATIONS AND DATA REDUCTION

In this work, we consider the time averaged *XMM-Newton* EPIC-pn spectra from the longest available observations of sources with a rate ≥ 0.5 counts/s in the X-ray band. The datasets were obtained through the *XMM-Newton* public data archive. The EPIC-pn camera has a higher effective area than the EPIC-MOS cameras, and drives the results of any joint spectral analysis. The reduction and analysis reported in this work used SAS version 8.0.0. We checked for pile-up in all the observations and found that this was not significant (i.e. less than 5 per cent for the high energy channels) for all the observations.

In Table 1 we present a log of the observations. We applied

the standard time and flare filtering (rejecting high-background periods of rate ≥ 0.4 counts/s, as recommended for the pn camera²). We filtered the event files, selecting only the best-calibrated events (pattern ≤ 4 for the pn), and rejecting flagged events (flag = 0).

For each exposure, we extracted the flux from a circular region on each source. The background was extracted from a circular region, not far from the sources. Both the coordinates of the centroids and the radius used for the regions were the same as those employed by Gladstone et al. (2009). We built response functions with the SAS tasks *rmfgen* and *arfgen*. We fitted the background-subtracted spectra with standard models in XSPEC 12.5.0 (Arnaud 1996). All errors quoted in this work are 90% confidence errors, obtained by allowing all variable parameters to float during the error scan. Owing to the uncertainties in the EPIC calibration, we used only the 0.3–10 keV range. The resulting spectra were grouped with the FTOOL *grppha* to bins with a minimum of 20 counts each.

3 SPECTRAL ANALYSIS AND RESULTS

In contrast to previous work, where Comptonization models are used to fit the data, we looked at the observations of NGC 1313 X-1, NGC 1313 X-2, M81 X-6, HOLM IX X-1, NGC 5408 X-1 and HOLM II X-1 from the point of view of a broad iron emission line, i.e. a reflection spectrum. An absorbed powerlaw was fitted to the data in the bands 1.2–3 and 8–10 keV. In the case of NGC 1313 X-2 and M81 X-6 we used the energy range 1–2 and 8–10 keV instead. The ratio of the whole 0.3–10 keV data set to the absorbed powerlaw is shown in Figure 1. The column densities found are in the range of $N_H = (0.1 - 0.5) \times 10^{22} \text{ cm}^{-2}$, thus larger than the corresponding galactic Hydrogen column densities (Dickey & Lockman 1990), indicating the presence of either local extra-absorption to the sources or intrinsic to the host galaxies. A large skewed emission feature, similar to those found in BHB and AGN (Miller et al. 2007; Tanaka et al. 1995; Nandra et al. 2008) is evident about 3 and 8 keV, and a soft excess (like those found in AGN) below 1 keV.

The data between 1.5 and 10 keV were then modelled with a powerlaw and a relativistic emission line (Laor 1991). A good fit is obtained with $\Gamma = 1.5 - 3$ (see Table 2). The addition of this line represents an improvement in the statistics of $\Delta\chi^2 = 60, 115, 367, 103, 65, 10$ (for 5 extra d.o.f.) for NGC 1313 X-1, NGC 1313 X-2, M81 X-6, HOLM IX X-1, NGC 5408 X-1 and HOLM II X-1, respectively. The line was thereafter significant in all the sources with exception of HOLM II X-1. HOLM II X-1 has the lowest *laor* line detection, due to both the short exposure time and steepness of the spectrum (we will refer to this point later). Further longer exposure observations of HOLM II X-1 are needed to fully address this point. Notice that no extreme inclination is required to reproduce the spectral drop ($\approx 40 - 60^\circ$). The strength of the line (equivalent width), the rest frame energy and the emissivity index of the line are in the range of $EW = 0.15 - 1.27$ keV, $E = 6.4 - 6.97$ keV and $q = 6 - 10$ (see Table 2). For the case of NGC 1313 X-1, NGC 1313 X-2, M81 X-6 and HOLM IX X-1 the rest-frame energies imply that we are dealing with ionized reflectors (the steepness of the powerlaw for the case of NGC 5408 X-1 and HOLM II X-1 did not allow us to obtain reliable values for the line parameters). There are remarkable emission line spectral features around $E \approx 0.6$ and 1 keV in the spectra of NGC 5408 X-1 and HOLM II X-1 (see Figure 1), which seem likely to come from

¹ It has to be noted that similar values, i.e. $kT_e = 1 - 3$ keV and $\tau \geq 5$, have been found in the description of the spectra of BHB during the *steep powerlaw* state (e.g. GRO J1655-40 and GRS 1915+105; Makishima et al. 2000; Kubota & Done 2004; Ueda et al. 2009).

² Information provided at "node52.html" of the User Scientific Guide.

Table 1. *XMM-Newton* observations log and effective exposure times of *XMM-Newton* instruments.

Source	Obs ID	Date	Exposure time (s)	Rate (counts s ⁻¹)
NGC 1313 X-1	0405090101	2006-10-16	121 212	0.73
NGC 1313 X-2	0405090101	2006-10-16	121 212	0.67
HOLM IX X-1	0200980101	2004-09-26	117 023	1.54
NGC 5408 X-1	0302900101	2006-01-15	130 549	0.96
M81 X-6	0111800101	2001-04-23	132 663	0.48
HOLM II X-1	0200470101	2004-04-15	104 677	3.13

O VIII K and Fe XVII and XVIII L. These lines have been usually understood as coming from the hot diffuse gas around these sources and/or emission from a photoionized stellar wind, similar to what is seen in some high-mass X-ray binaries in our own Galaxy (Feng & Kaaret 2005; Stobbart et al. 2006). Goad et al. (2006) argued that these features commonly seen in the spectra from ULX correspond to poorly modeled spectra of ULX considering absorbers with solar metal abundances (i.e. they instead found that the RGS spectrum of HOLM II X-1 is consistent with an absorber of 0.6 times solar abundance). Nevertheless, this value does not mean anything about the local environment of the source, since this is the metal abundance found in the total galactic column density in the direction to the source³. As pointed by Ross & Fabian (2005), these lines can plausibly come from the disk of the sources. They originate through X-ray ionized reflection, which occurs when a surface is irradiated with X-rays. The reflection continuum is then complex and needs to be modelled properly.

3.1 Reflection spectra

We have therefore fitted Ross & Fabian (2005) ionized reflection models to the whole 0.3–10 keV observable band. Very good agreement is obtained with a model which is relativistically blurred, has supersolar abundances between 4 and 10 and photon index of $\Gamma \approx 1.5 - 1.6$ for NGC 1313 X-1, NGC 1313 X-2 and HOLM IX X-1, $\Gamma \approx 2$ for M81 X-6 and steeper ($\Gamma \geq 2.5$) for NGC 5408 X-1 and HOLM II X-1 (see Table 2). In the case of NGC 5408 X-1 and HOLM II X-1, this model has worse statistics ($\chi^2/\nu = 736/577, 945/779$), presumably due to the steepness of the spectrum, which makes the statistics be dominated by the softest part of the spectrum ($E \leq 1.5$ keV). This would make easy the determination of the O abundance (because the lowest part of the spectrum is very well sampled) at the expense of having Fe badly constrained (being responsible for the emission at the highest part of the spectrum). Nevertheless, a study with variable abundances is beyond the scope of this paper. This model provided a good description of the data (see Table 2). The ionization parameter of the reflection model is in the range of $\xi = 29 - 2500$. The high values found for the ionization parameter for NGC 1313 X-1, NGC 1313 X-2, M 81 X-6 and HOLM IX X-1 are very likely related to the featureless low energy ($E \leq 1$ keV) spectra for these sources.

The relativistic blurring is accomplished using a Kerr kernel (Laor 1991) with a radial emissivity index in the range of $q = 4 - 9$ (where the emissivity has the radial dependence r^{-q}) from $R_{in} = 1.2 - 1.4 R_g$ for NGC 1313 X-1, NGC 1313 X-2 and M81 X-6 and $R_{in} = 2.0 - 2.5 R_g$ for HOLM IX X-1, NGC 5408 X-1 and

HOLM II X-1. Here, $1R_g = GM/c^2$. The outermost radius is fixed to $400 R_g$, a canonical value inferred from fits to spectra of AGNs. Since there is no previous measurement for the inner disk inclination so far, it was constrained in the fits to be within the range of $i = 40 - 60^\circ$, i.e. an intermediate value. The inner disk radii found for the former ones indicate that the matter reaches the last stable orbit for a very rapidly spinning black hole, as inferred from the highly skewed profiles for the broad Fe K line for these sources (see Figure 1). They show very strong reflection components as well ($F_{refl}/F_{total} = 0.7 - 1$), i.e. the spectrum is dominated by reflection, thus being *reflection-dominated* sources. Indeed, NGC 1313 X-2 and M81 X-6 are the most extreme cases, with no signs of emission from a powerlaw high-energy source. In contrast, for the cases of HOLM IX X-1, NGC 5408 X-1 and HOLM II X-1, the spectra are powerlaw dominated (*powerlaw-dominated* sources). Curiously, the reflection dominated sources are the ones which show the smallest inner disk radii, perhaps indicating that light bending is an important effect for them. It is worth noting that for the most *reflection-dominated* sources, i.e. NGC 1313 X-2 and M81 X-6, the residuals at the broad Fe complex look peaky and that this is a natural consequence of the fact that we are modelling with a uniform disk, which could differ in properties to its outer region⁴. In contrast, for the powerlaw dominated sources, the inner disk radii are larger. In the case of HOLM IX X-1, the larger radius ($R_{in} = 2.0 R_g$) is accompanied by the flattest powerlaw in the overall sample ($\Gamma = 1.504 \pm 0.004$), and this could imply that reflection occurs farther from the black hole with respect to the reflection dominated ones. In the case of NGC 5408 X-1 and HOLM II X-1, with steeper powerlaw indices ($\Gamma \geq 2.5$) and showing worse fit statistics, due to the lower signal-to-noise of the high-energy channels, no definite statements can be made. In none of the spectra does the addition of a disk component (diskbb in XSPEC) improve the statistics. Therefore, we conclude that we cannot detect thermal emission from the disk for these sources (we shall return to this point in Section 4).

The fits with both the laor and the reflection models above indicate high values of the emissivity parameter ($q = 4 - 9$), indicating that relativistic blurring is an important effect and the emission is concentrated near the innermost radii. The respective inner disk radii obtained are low ($R_{in} = 1.25 - 2.5 R_g$), indicating X-ray emission from regions very close to the black hole, where strong light bending dominates. These effects mean that high values of the spins of the black holes are expected. To study this possibility further, we substituted the Kerr kernel (kdblur), which assumes maximal spin, by the relativistic kernel of (kerrconv;

³ In this paper we apply a model describing the X-ray emission local to the source which incorporates the metal abundances as a parameter, thus potentially allow us to unveil the metallicities local to these sources.

⁴ The emissivity parameter is expected to vary between the inner and the outer boundaries of the disk, giving very smooth (high q) and peaky (low q) components, respectively. In this paper we just model the smooth component, expected to come from the inner region of the disk.

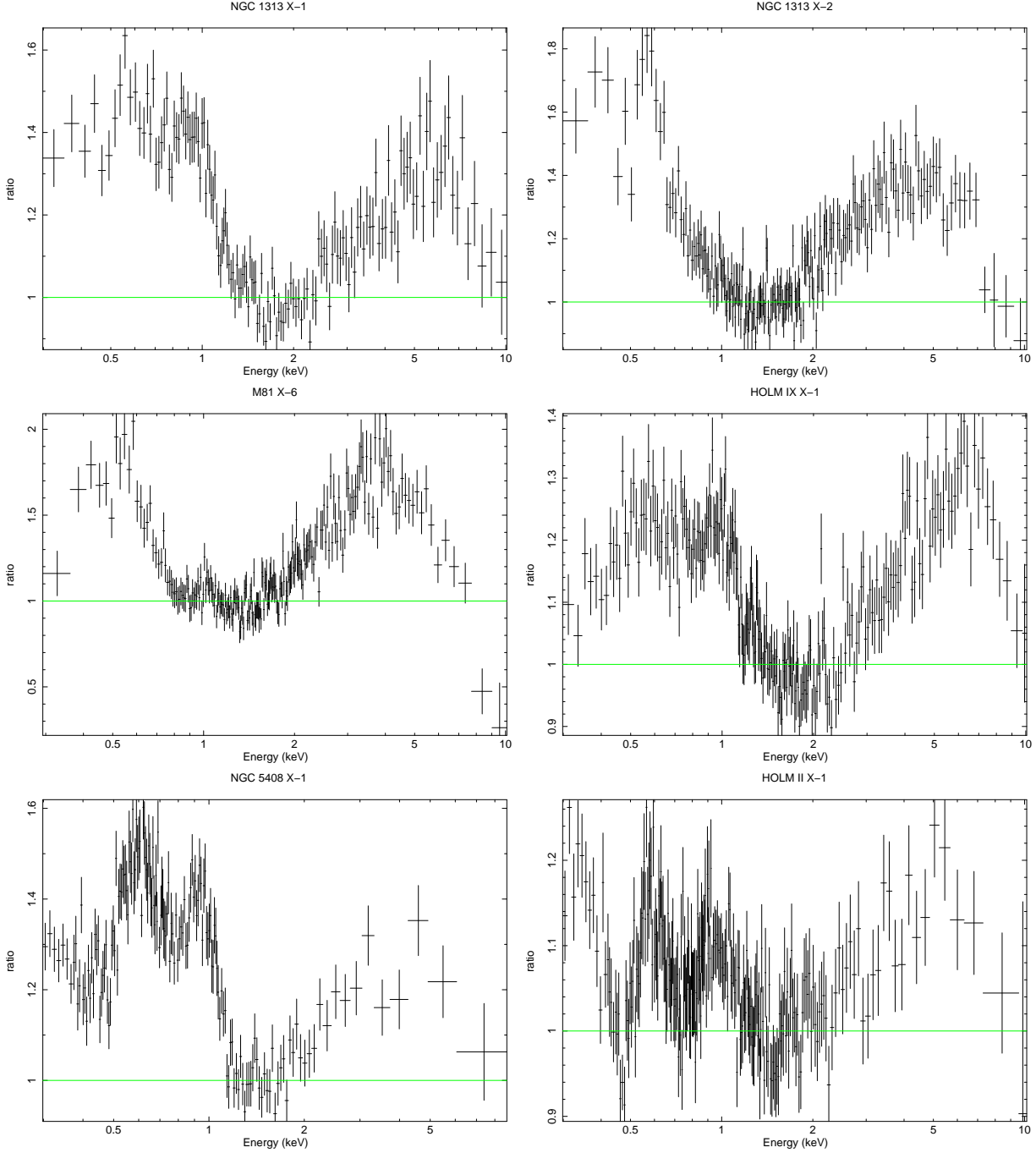


Figure 1. Ratio of the *XMM-Newton* pn spectra of NGC 1313 X-1, NGC 1313 X-2, M81 X-6, HOLM IX X-1, NGC 5408 X-1 and HOLM II X-1 (upper-left to lower-right) to the powerlaw which fits best between 1.2–3 and 8–10 keV. A broad iron line and a soft excess are evident. Data have been rebinned for visual clarity.

Brenneman & Reynolds 2006), which assumes variable spin parameter ($a = cJ/GM^2$; where J is the angular momentum of a black hole of mass M). We assumed the inner disk radii to be equal to the marginal stability radius (i.e. the closest inner disk radius to the black hole) and constrained the disk inclination to an intermediate value ($i = 40 - 60^\circ$). Thanks to the flat spectra of NGC 1313 X-1, NGC 1313 X-2, M 81 X-6 and HOLM IX X-1, which lead to a strong signal at high energies, we could constrain well the values of the emissivity parameter of the disk and the spin of the black hole. The spins for the black holes of these sources are very high, and

close to the value of a maximal spinning black-hole ($a = 0.998$), with M 81 X-6 hosting the most rapidly spinning black hole of the sample ($a = 0.993 - 0.998$). In the case of HOLM II X-1, the lowest value found ($a = 0.47 \pm 0.12$) might be a consequence of the steep powerlaw and short exposure, which lead to little high-energy signal (NGC 5408 X-1 is similar). Future work is needed in order to fully address this point. As in the application of the Kerr kernel, the values obtained for the ionization parameters are higher for NGC 1313 X-1, NGC 1313 X-2, M 81 X-6, HOLM IX X-1 than in NGC 5408 X-1, HOLM II X-1, which correspond to featureless

low-energy spectra for the former ones due to the current exposure times used. The opposite occurs for NGC 5408 X-1 and HOLM II X-1, for which we could constrain very well the ionization parameter (i.e. the disk density) to $\xi = 49.4 \pm 0.8, 29 \pm 6$, due to the good signal of the spectrum at low energies ($E \leq 1.5$ keV). This value is low for both sources and indicates a high density for the reflecting medium (i.e. the disk).

For all the sources, we find that iron is overabundant compared to the Sun by 4 – 9 times. Usually, ULX have been associated with metal poor environments, because stars in these sites lose less mass during their evolution and can reach very high masses and collapse to high-mass black holes ($M \leq 80 M_{\odot}$) at the end of their lives (Fryer & Kalogera 2001). Furthermore, there is observational evidence of real low-metal abundances in the galaxies which host these ULX. Metal abundance measurements from the HII regions in NGC 1313 and HOLM II X-1 have values $Z \approx 0.008, 0.1$ (Hadfield & Crowther 2007; Pakull & Mirioni 2002) and Mapelli et al. (2009) have found similar values for other ULX host galaxies. These facts agree with the known mass-metallicity relation, in which the smallest galaxies are the poorest in metals. Winter et al. (2007) found metal overabundance for a sample of ULX, with mean metallicity close to the solar value⁵. With exception of HOLM II X-1 and HOLM IX X-1, where the metal abundance they obtain is compatible with ours, we can explain the discrepancy in the level of metals by means of the different model used for the soft excess (thermal emission from an accretion disk in their case). Nevertheless, they found, like in our study, that the galaxies do not obey the mass-metallicity relation in X-rays. This does not mean a conflict with optical measurements, since we are measuring metallicities local to the sources in X-rays. One possible scenario to explain such high values for the metallicities observed local to the sources, without any apparent chemical metal enrichment in their surrounding environments, is that the metals were blown out by the type II SNe event and then recaptured (similar to the fallback disk model of Li 2003). We shall return to this point later in Section 4.

4 DISCUSSION

Remarkably, a relativistically-blurred, reflection-dominated model gives a very good fit to the sample of ULX with best quality (100 ks of time exposure) *XMM-Newton* data. Very skewed iron line profiles have been found, implying that the emission region is very close to the black-hole and this fact allowed us to determine their spin. We find that all the ULX in our sample are close to maximally rotating, with the exception of NGC 5408 X-1 and HOLM II X-1, for which the steep powerlaw did not allow us to properly determine parameters from the Fe line. We have found that, the sources showing a *reflection dominated* spectrum (NGC 1313 X-1, NGC 1313 X-2 and M 81 X-6) have maximally spinning black-holes. This fact can be understood if light bending is an important effect for these sources. For these sources, the high-energy source (i.e. the jet or corona) is very close to the black hole and the observed direct continuum (i.e. powerlaw) is very low. This would correspond to Regime I of Miniutti & Fabian (2004), corresponding to a low height of the primary source, where strong light suffered by the primary radiation dramatically reduces the observed

powerlaw emission component at infinity. HOLM IX X-1 shows a *powerlaw dominated* spectrum with a slightly narrower Fe line profile. This would correspond to Regime II of Miniutti & Fabian (2004), when the height of the primary source is larger, and the observed direct continuum (i.e. powerlaw) stronger. The line profile is narrower than in regime I because the emissivity profile of the disk is flatter, as result of a nearly isotropic illumination. For NGC 5408 X-1 and HOLM II X-1, we find a clear reflection component but the steepness of the spectra means that the Fe K features are less well-measured.

The spectral solution we have found here for ULX suggests a new explanation for accretion onto spinning black holes. Our model assumes that the dominant source of radiation is a power-law continuum produced a few gravitational radii above a rapidly spinning black hole. Little thermal radiation is produced by the disc and is undetected by the current data. We assume that the power for this source is extracted magnetically from the disc and transferred to the emission region by magnetic fields. Some of the power may even be extracted magnetically from the spin of the black hole (Blandford & Znajek 1977). Since radiation is only produced above the disc, radiation pressure need not oppose accretion. Indeed it will help squash the disc and maintain the high surface density required for our relatively low ionization parameters and thus observable reflection. (Note that strong light bending occurs in the region being considered which is very close to a black hole, meaning that there is beaming but in the opposite sense to that normally envisaged.)

The relevant radiation for computing the physical Eddington limit in this situation is the thermal disc radiation, not the power-law continuum and reflection associated with it. Since we detect no such thermal radiation, then the situation may be sub-Eddington, even for stellar mass black holes. Whether this solution can work depends on the extent to which magnetic energy extraction can be clean, in the sense of not requiring considerable thermal energy release. We note that the accretion flow is super-Eddington in the conventional interpretation in which the total energy release is considered (especially since some radiation falls straight into the black hole).

If the above solution is appropriate for these objects then they can either be stellar mass black holes with masses of $\approx 10 M_{\odot}$ or IMBH of $100s M_{\odot}$. Their spin is then likely to be natal. If they form through stellar collapse and the progenitor star was highly spinning, then it would be likely that the black hole would remain highly spinning. Many studies have argued that a binary companion can spin up a massive star but the magnitude of the spin up is still a matter of debate (e.g., Paczynski et al. 1998; Fryer 1999; Brown et al. 2000). Accretion would presumably come from a binary companion. An interesting alternative is that they accrete from a debris disc produced by fallback from the (failed) supernova or collapsar (Li 2003). This could account for the high metallicity we infer (note that hydrogen-poor accretion would also slightly raise the Eddington limit).

In summary, some ULX may consist of fast spinning black holes accreting rapidly from a metal-rich disc. Accretion power passes magnetically to the primary emission region which lies just outside the accretion flow. Strong reflection occurs, creating a soft excess and very broad iron-K features in the 0.3-10 keV X-ray spectrum. Sensitive hard X-ray spectra in the 10–50 keV band may test this scenario.

⁵ The sources with the longest exposure times in their observations, i.e. HOLM II X-1 and HOLM IX X-1 clearly are outliers of this relation.

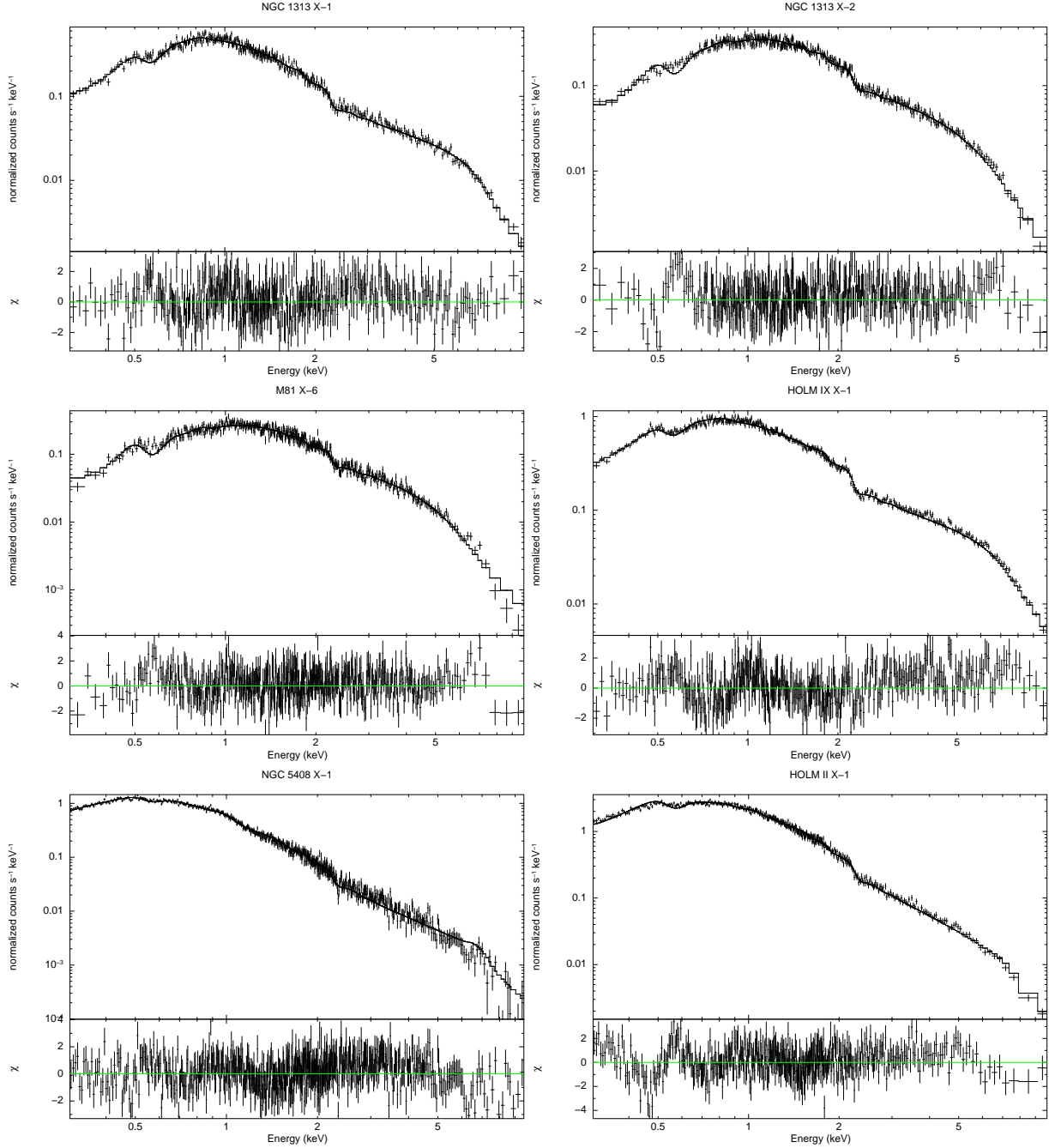


Figure 2. The best-fitting (blurred) ionized reflection plus power-law model plotted on the spectra of NGC 1313 X-1, NGC 1313 X-2, M 81 X-6, HOLM IX X-1, NGC 5408 X-1 and HOLM II X-1 (upper-left to lower-right). Simple photoelectric absorption has also been applied. The model fits the data very well over the entire observed energy band. Data have been rebinned for visual clarity.

ACKNOWLEDGMENTS

This work is based on observations made with XMM-Newton, an ESA science mission with instruments and contributions directly funded by ESA member states and the USA (NASA). We thank the anonymous referee for helpful comments.

REFERENCES

- Abolmasov, P., Fabrika, S., Sholukhova, O. & Afanasiev, V., 2007, *Astrophysical Bulletin*, 62, 36
- Arnaud, K. A., 1996, *Astronomical Data Analysis Software and Systems V*, ASP Conf. Ser., 101, 17
- Blandford, R. D. & Znajek, R. L., 1977, *MNRAS*, 179, 433
- Brenneman, L. W. & Reynolds, C. S., 2006, *ApJ*, 652, 1028
- Brown G E, Lee C-H, Wijers R A M J et al., 2000, *New Astronomy*, 5, 191
- Cackett, E. M., Miller, J. M., Bhattacharyya, S. et al., 2008, *ApJ*, 674, 415
- Colbert, E. J. M. & Mushotzky, R. F., 1999, *ApJ*, 519, 89
- Dewangan, G. C., Griffiths, R. E. & Rao, A. R., 2006, *ApJ*, 641L, 125

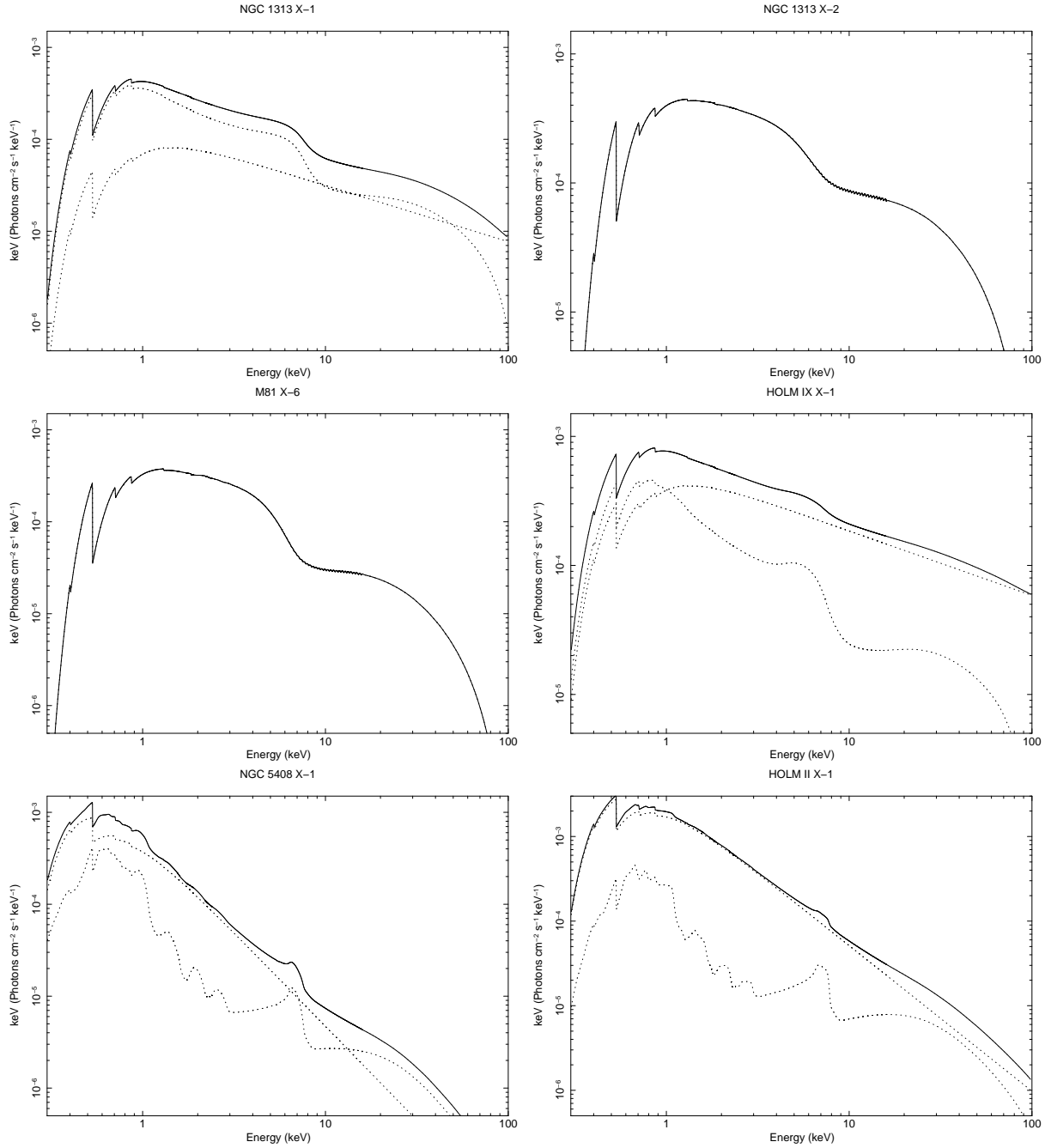


Figure 3. The (blurred) ionized reflection plus power-law model for NGC 1313 X-1, NGC 1313 X-2, M 81 X-6, HOLM IX X-1, NGC 5408 X-1 and HOLM II X-1 (upper-left to lower-right) used in the fits shown in Figure 2.

Dickey & Lockman, 1990, ARAA, 28, 215
 Fabian, A. C., Zoghbi, A., Ross, R. R. et al., 2009, Nature, 459, 540
 Fabbiano, G., 1989, ARA&A, 27, 87
 Fabbiano, G. & White, N. E., 2006, *Compact stellar X-ray sources in normal galaxies*, Cambridge Univ. Press, 475
 Feng, H. & Kaaret, P., 2005, 2005, ApJ, 633, 1052
 Fryer C. L., 1999, ApJ, 522, 413
 Fryer, C. L. & Kalogera, V., 2001, ApJ, 554, 548
 George, I. M. & Fabian, A. C., 1991, MNRAS, 249, 352
 Gladstone, J. C., Roberts, T. P. & Done, C., astro-ph/0905.4076
 Goad, M. R., Roberts, T. P., Reeves, J. N. & Uttley, P., 2006, MN-

RAS, 365, 191
 Guilbert, P. W. & Rees, M. J., 1988, MNRAS, 233, 475
 Hadfield, L. J. & Crowther, P. A., 2007, MNRAS, 381, 418
 Kaaret, P., Ward, M. J. & Zezas, A., 2004, MNRAS, 351L, 83
 Karachentsev, I. D., Sharina, M. E., Dolphin, A. E. et al., 2002, A&A, 385, 21K
 King, A. R., 2002, MNRAS, 335, 13L
 Kubota, A. & Done, C., 2004, MNRAS, 353, 980
 Laor, A., 1991, ApJ, 376, 90
 Li, X.-D., 2003, ApJ, 596L, 199
 Liu, J. & Di Stefano, R., 2008, ApJ, 674L, 73
 Makishima, K., Kubota, A., Mizuno, T. et al., 2000, ApJ, 535, 632

Table 2. Spectral parameters from fits with the laor and the reflection model.

Parameter	NGC 1313 X-1	NGC 1313 X-2	M 81 X-6	HOLM IX X-1	NGC 5408 X-1	HOLM II X-1
Laor Model						
E (keV)	6.79±0.18	6.87±0.10	6.85±0.13	6.91±0.06	6.48±0.08	6.4±0.7
EW (keV)	0.36	0.45	1.27	0.70	0.43	0.15
q	7.1±0.6	9.1±0.5	9.95±0.05	6.8±0.5	9.77±0.23	8.05±1.9
Γ	1.77±0.03	2.02±0.05	2.56±0.02	1.57±0.02	2.94±0.09	2.61±0.03
χ^2/ν	645/680	709/711	646/599	1 000/1 036	380/335	578/539
Blurred Reflection Model						
N_H (10^{22} cm $^{-2}$)	0.241±0.002	0.374±0.003	0.422±0.004	0.164±0.002	0.129±0.001	0.179±0.003
Γ	1.627±0.013	1.504±0.005	2.043±0.012	1.504±0.004	3.04±0.01	2.72±0.01
q	4.61±0.07	9.02±0.10	8.72±0.09	4.52±0.14	6.5±0.6	4.8±1.1
R_{in} ($R_g = GM/c^2$)	1.36±0.07	1.244±0.009	1.314±0.008	2.09±0.06	2.45±0.08	2.30±0.20
R_{out} (R_g)	400	400	400	400	400	400
i (°)	44.0±0.7	46.2±0.4	40.31±0.19	50±10	55.7±0.5	59.5±0.5
Fe/solar	7.1±0.3	7.7±0.5	9.6±0.4	4.98±0.12	4.06±0.12	4.5±0.8
ξ ($= 4\pi F_{\text{irr}}/n$)	2 155±12	2 531±13	1 789±14	1 673±19	49.4±0.8	29±6
$F_{\text{powerlaw}}/F_{\text{total}}$ ^a	0.32	— ^b	—	0.77	0.75	0.92
χ^2/ν	975/919	991/952	956/840	1 292/1 275	736/577	945/779
$L_{(0.05-100)\text{ keV}}$ (erg s $^{-1}$)	1.4×10 ⁴⁰	2.1×10 ⁴⁰	1.9×10 ⁴⁰	3.6×10 ⁴⁰	6.7×10 ⁴⁰	1.4×10 ⁴¹
a ($= cJ/GM^2$)	0.960 – 0.998	0.970 – 0.998	0.993 – 0.998	0.95±0.17	0.70 ^{+0.12} _{-0.05} ^c	0.47±0.12 ^d

^a Fluxes calculated in the 0.05–100 keV energy band.^b For NGC 1313 X-2 and M 81 X-6 the best fits were obtained considering fully reflection dominated models, i.e. $F_{\text{powerlaw}}/F_{\text{total}} = 0$.^c *kerrconv* gave a worse fit (755/578) than *kdblur* for this source.^d *kerrconv* provides a fit of the same quality (945/779) as *kdblur* (see text).

Mapelli, M., Colpi, M. & Zampieri, L., 2009, MNRAS, 395L, 71
 Miller, J. M., Fabbiano, G., Miller, M. C. & Fabian, A. C., 2003, ApJ, 585L, 37
 Miller, J. M., Fabian, A. C. & Miller, M. C., 2004, ApJ, 607, 931
 Miller, J. M., 2007, ARA&A, 45, 441
 Miller, M. C. & Colbert, E. J. M., 2004, International Journal of Modern Physics D, 13, 1
 Miniutti, G. & Fabian, A. C., 2004, MNRAS, 349, 1435
 Miyawaki, R., Makishima, K., Yamada, S., et al., 2009, PASJ, 61S, 263
 Nandra, K., O’Neill, P. M., George, I. M. & Reeves, J. N., 2007, MNRAS, 382, 194
 Paczynski B., 1998, ApJ, 494, L45
 Pakull, M. W. & Mirioni, L., 2002, *Optical Counterparts of Ultraluminous X-Ray Sources*, astro-ph/0202488
 Pakull, M. W. & Mirioni, L., 2003, *Bubble Nebulae around Ultraluminous X-Ray Sources*, Revista Mexicana de Astronomía y Astrofísica Conference Series, Eds. Arthur, J. & Henney, W. J., 15, 197
 Reis, R. C., Fabian, A. C., Ross, R. R. et al., 2009a, MNRAS, 395, 1257
 Reis, R. C., Fabian, A. C. & Young, A. J., 2009b, astro-ph/0904.2747
 Remillard, R. A., McClintock, J. E., 2006, ARA&A, 44, 49
 Roberts, T. P., Warwick, R. S., Ward, M. J., 2005, MNRAS, 357, 1363
 Roberts, T. P., 2007, Ap&SS, 311, 203
 Ross, R. R. & Fabian, A. C., 2005, MNRAS, 358, 211
 Soria, R., Fender, R. P. et al., 2006, MNRAS, 368, 1527
 Stobbart, A.-M., Roberts, T. P. & Wilms, J., 2006, MNRAS, 368,

397
 Strohmayer, T. E., Mushotzky, R. F. et al., 2007, ApJ, 660, 580
 Tanaka, Y., Nandra, K., Fabian, A. C., et al., 1995, Nature, 375, 659
 Ueda, Y., Yamaoka, K. & Remillard, R., 2009, ApJ, 695, 888
 Winter, L. M., Mushotzky, R. F. & Reynolds, C. S., 2007, ApJ, 655, 163